A Theoretically Based Valve Noise Prediction Method for Compressible Fluids

G. Reethof
Professor of Mechanical Engineering and Director of Noise Control Laboratory. Fellow ASME

W. C. Ward
Graduate Assistant.

Dept. of Mechanical Engineeirng, The Pennsylvania State University, University Park, PA 16802

Noise generated by control valves in power generation, chemical and petrochemical plants must be predictable so that proper design measures can be taken to conform to OSHA's noise regulation. Currently available noise prediction methods are empirically based and not sufficiently accurate. The method proposed is based on jet noise theory for both subcritical and choked conditions, duct acoustics theory in terms of higher order mode generation and propagation, and the theory of acoustics-structure interaction in the development of the transmission loss values for the pipe. One third octave values are calculated over the audio spectrum by incorporating spectral aspects of noise generation, propagation, transmission, and radiation. The predicted values of noise for several size cage globe valves over wide pressure ranges compare well with measured results by two prominent valve manufacturers. The method, at present, is restricted to conventional valve styles, as opposed to the special low noise valve types with their very complicated orificial elements.

Introduction

The noise generated by control valves and regulators in chemical, petrochemical, and steam power plants has received much attention over the last 10 years because of the potential health and communication hazards to workers inside the plants and the objectionable noise levels which are radiated into surrounding communities. Typical noise levels inside large stream power plants can range up to 120 dBA in the vicinity of the large piping arrangements. Such levels are in excess of the OSHA limits for typical exposures of workers.

The valve industry has responded to this problem by, on the one hand, developing valve noise prediction methods to aid the plant designers, and on the other hand, developing quieter valves which are based on concepts of multiple series and parallel expansion or tortuous path approaches. However, such quiet valves are far more complex than conventional valves, such as globe, butterfly, and simple trim configurations, and may cost as much as 10 times more and, in several instances, result in reduced reliability.

Most attention has been given to the aerodynamically generated noise situations, since the dominant noise generation process in the hydrodynamic case is cavitation. Cavitation almost always is accompanied by serious physical damage to the metering elements in the valve, due to cavitation erosion. Properly designed and used valves with liquids avoid cavitation conditions. This paper, therefore, deals only with aerodynamically generated noise. A discussion of the background to valve noise prediction, with an extensive bibliography, is given in references [1] and [2]. At the present time, each valve manufacturer has developed its own valve noise prediction method. The methods are largely based on the results of measurements on many valves, over a limited range of sizes, and with only air, at ambient temperatures, as the fluid. Some valve companies have attempted to develop methods based on free jet noise theory, with only limited success. Therefore, the accuracy of these prediction methods is not satisfactory, particularly if the methods are applied to valves larger than those tested and if the valve's throttling element geometries differ from prior experience. The reasons for these difficulties will become apparent from the discussion of the various elements that enter into prediction methods. A recent study of the variation in noise prediction using various manufacturers' methods [3] illustrates the present, not fully satisfactory, state of affairs.

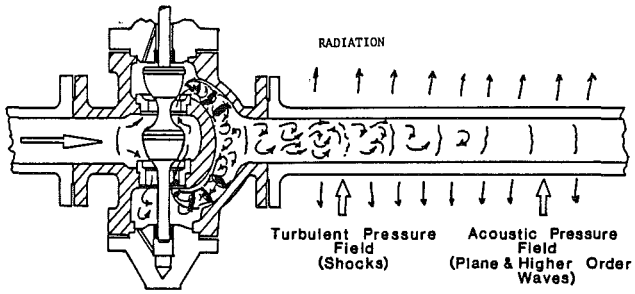

Fig. 1 Schematic representation of valve noise generation, propagation, transmission, and radiation

A recently published method by Dr. H. D. Baumann [4], representing many years of pioneering work, does appear promising. Certain facets of this work have been incorporated into the method presented in this paper. Dr. Baumann's work is based on the concept of an acoustic efficiency η as a function of pressure recovery F_L, pressures across the valve, a siz-

Contributed by the Noise Control and Acoustics Division for publication in the JOURNAL OF VIBRATION, ACOUSTICS, STRESS, AND RELIABILITY IN DESIGN. Manuscript received at ASME Headquarters, January 7, 1986.

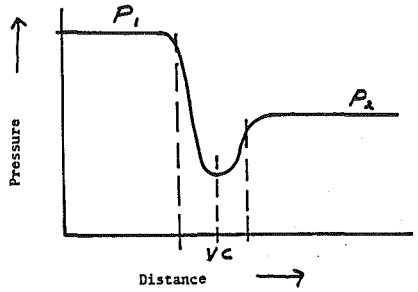

Fig. 2 Typical pressure recovery characteristics downstream of valves

ing coefficient and gas properties. The method does not incorporate several features, related to the acoustics inside the pipe and the pipe wall transmission, which are important for a general method.

The construction of valves results almost always in rigid, massive valve bodies, which do not radiate significant acoustic energy. The propagation of sound upstream from the valves, even for subcritical pressure ratios, is not a serious problem.

The processes associated with noise from valves and the associated piping can be broken down into four interrelated elements, which are pictured in Fig. 1: (1) the noise generation processes just downstream of the throttling elements which are either turbulent shear dominated or shock cell–turbulence interaction dominated; (2) the development of the acoustic field inside the piping downstream of the valves; (3) the excitation of the pipe wall vibrations; and (4) the radiation of the sound into the space surrounding the downstream pipe.

In order to approach the development of prediction methods, analytical relationships which describe these four processes must be developed. Considerable progress has been made over the last several years. Support of research at Penn State University by the National Science Foundation over several years and by several valve companies, as well as the efforts of the Instrument Society of America's Valve Noise Prediction Task Force, has permitted this progress.

Sound Power Determination

Control valves are pressure-reducing devices controlling pressure or flow by throttling the fluid in the orificial elements. For subcritical pressurization, the noise is generated by the intense turbulent mixing of the high-velocity spatially complex jet, or several jets, emanating from the throttling elements. Pressure recovery, as shown schematically in Fig. 2, occurs in this mixing region because of the recirculating flows that are generated in the continued jet mixing process. Therefore, the noise generation process can not simply be treated as a free subsonic jet by applying the extensive jet noise research results related to jet engines. The pressure recovery coefficient F_L is defined [5] by:

$$F_L{}^2 = \frac{P_1 - P_2}{P_1 - P_{vc}} \tag{1}$$

The pressure recovery characteristics of various valve styles are determined by their orifical geometry, the valve opening and valve gallery configuration. Thus, cage globe valves have low pressure recoveries ($F_L = 0.95$) and butterfly valves have large pressure recoveries ($F_L \approx 0.5$). A corollary of high-pressure recovery is that sonic velocities will be reached at lower pressure ratios than for the case of no recovery. The critical pressure ratio for isentropic flow to the vena contracta is given by

Nomenclature

a = speed of sound, m/s
A_j = jet area, m^2
A_{vc} = vena contracta area, m^2
C_v = valve flow coefficient
d = outside diameter of pipe, m
D_j = effective diameter of valve orifice, m
E = pipe wall material, modulus of elasticity, N/m^2
E_2 = acoustic energy inside the pipe, N – m/s
E_o = acoustic energy outside the pipe, N – m/s
f = frequency, Hz
f_i = one-third octave band center frequencies, Hz
F_d = trim coefficient
F_L = pressure recovery coefficient
$G(M)$ = velocity correction factor
K = stiffness, N/m
k_{mn} = radial wave number of mth circumferential and nth radial mode, 1/m
k = wave number ω/a_2, 1/m
k_x = free space axial wave number, 1/m
k_{xs} = shell axial wave number (pipe), 1/m
L_w = sound power level, dB
[L] = matrix differential operator given in Appendix A
L_{TL} = pipe wall transmission loss, dB
L_a = A weighted sound pressure level at outer pipe wall, dB
L_s = A weighted sound pressure level at distance s from pipe, dB
m = circumferential mode number (acoustic or pipe flexural)
m_e = mass of a pipe element, kg
M = convection flow Mach number in downstream pipe
n = radial acoustic mode number
n_o = apparent number of noise producing orifices
P = absolute pressure, N/m^2
p = RMS acoustic pressure, N/m^2
R_m = mechanical resistance of pipe
r = radial dimension in cylindrical coordinates
r_p = pipe internal radius, m
R = mean pipe radius
s = distance from centerline of pipe, m
S_n = Strouhal number, Hz/Hz
h = pipe wall thickness, m
$\{U_i\}$ = displacement vector in the u, v, w coordinates which are orthogonal in the r, θ, and x directions
V_j = jet velocity, m/s
W_{ac} = acoustic power, W
x = axial dimension in cylindrical coordinates
X = mechanical reactance of pipe
ϵ = dimensionless parameter $t\,k_x$
β = dimensionless parameter h/R
γ = ratio of specific heats
η_s = material loss factor (10^{-4} for steel)
θ = circumferential angle in cylindrical coordinates
σ = internal radiation efficiency
σ_o = external radiation efficiency
ν = pipe wall material, Poisson's ratio
ρ_j = fluid density in emerging jet, kg/m^3
ρ_o = external fluid mass density, kg/m^3
ρ = internal fluid mass density, kg/m^3
ρ_s = pipe wall material mass density, kg/m^3
Ω = dimensionless parameter $\omega t\sqrt{\rho(1-\nu^2)/E}$
$\Delta\omega_i$ = frequency bandwidth, rad/s
ω = frequency, rad/s
α = pressure ratio correction for recovery

Subscripts

1 = upstream condition
2 = downstream condition
vc = vena contracta condition

$$\left(\frac{P_{vc}}{P_1}\right)_{\text{crit}} = \left(\frac{2}{\gamma+1}\right)^{\frac{\gamma}{\gamma-1}} \tag{2}$$

Equation (1) can be combined with equation (2) to arrive at a critical pressure ratio in terms of P_2, P_1, F_L, and γ.

$$\left(\frac{P_2}{P_1}\right)_{\text{crit}} = 1 - F_L{}^2\left[1 - \left(\frac{2}{\gamma+1}\right)^{\frac{\gamma}{\gamma-1}}\right] \tag{3}$$

The case of $F_L = 0.75$ and air ($\gamma = 1.4$) gives a critical pressure ratio of $P_1/P_2 = 1.36$, compared to 1.89 for no recovery [4]. Thus, higher recovery valves choke at lower pressure ratios than low recovery valves.

Research on simple orifices and valves followed by sections of straight pipe has shown that the noise generation process is dominated by dipole type acoustic sources [6]. Because of the "compact" nature of the internal radiating surfaces and the higher efficiencies of dipole radiators compared to the quadrupoles, which dominate the noise generation in free jets, the dipole sources dominate the noise from confined jets. The sound power W_{ac} generated by dipoles is given by the following proportionality

$$W_{ac} \propto \rho_j V_j{}^6 A_j a^{-3} \tag{4}$$

Since the region of highest velocity for subsonic flow is at the vena contracta, the sound power generated will be dominated by that condition. The velocity in the vena contracta and the resulting Mach number are given by the following relationships for isentropic flow (assuming $V_1 << V_{vc}$):

$$V_{vc}^2 = \left[2\left(\frac{\gamma}{\gamma-1}\right)\frac{P_1}{\rho_1}\left\{1 - \left(\frac{P_{vc}}{P_1}\right)^{\frac{\gamma-1}{\gamma}}\right\}\right] \tag{5}$$

$$a_{vc} = a_2\left(\frac{P_{vc}}{P_1}\right)^{\frac{\gamma-1}{2\gamma}} \tag{6}$$

$$M_{vc}^2 = \left(\frac{V_{vc}}{a_{vc}}\right)^2 = \frac{2}{\gamma-1}\left[\left(\frac{P_1}{P_{vc}}\right)^{\frac{\gamma-1}{\gamma}} - 1\right] \tag{7}$$

The flow area in the vena contracta A_{vc} is related to the value's flow coefficient C_v and F_L defined by

$$A_{vc} = \frac{C_v F_L}{59{,}055}\ [m^2] \tag{8}$$

The sound power generated by the turbulent shear mechanisms in the subsonic flow regime becomes:

$$W_{ac} = 1 \times 10^{-9} a_2{}^2 M_{vc}^6 C_v F_L \rho_1 \left(\frac{P_{vc}}{P_1}\right)^{\frac{1}{\gamma}} a_{vc} \tag{9}$$

The constant in equation (9) contains a reference acoustic to mechanical power conversion ratio for a sonic jet ($M_{vc} = 1$) of 3×10^{-4} which is the result of measurements by the authors and others. This reference "acoustic efficiency" is the only empiricism in the method.

Above the critical pressure ratio given by (3) the velocity in the vena contracta will remain sonic and stationary shock cells of increasing strength will appear as pressure ratio increases. Up to a certain pressure ratio given, by equation (10), the sound power as given by equation (11) continues to be dominated by turbulent mixing.

$$\frac{P_1}{P_2\alpha} = [0.754(\gamma + 0.326)]^{\frac{\gamma}{\gamma-1}} \tag{10}$$

$$W_{ac} = 1 \times 10^{-9} a_2{}^3 M_j^5 C_V F_L \rho_1 \left(\frac{2}{\gamma+1}\right)^{\frac{\gamma+1}{2(\gamma-1)}} \tag{11}$$

The vena contracta Mach number in equation (9) is replaced by the freely expanded jet Mach number M_j, which is given by:

$$M_j{}^2 = \frac{2}{\gamma-1}\left[\left(\frac{P_1}{P_2\alpha}\right)^{\frac{\gamma-1}{\gamma}} - 1\right] \tag{12}$$

The recovery correction factor α is given by (at the critical pressure ratio, $M_{vc} = M_j = 1$)

$$\alpha = \frac{(P_{vc}/P_1)_{\text{crit}}}{(P_2/P_1)_{\text{crit}}} = \frac{\left(\frac{2}{\gamma+1}\right)^{\frac{\gamma}{\gamma-1}}}{1 - F_L{}^2\left[1 - \left(\frac{2}{\gamma+1}\right)^{\frac{\gamma}{\gamma-1}}\right]} \tag{13}$$

Above the pressure ratio given by (10) and up to $M_j = \sqrt{2}$ (or $(M_j{}^2 - 1)^{1/2} = 1$), the sound power generated is dominated by the shock-cell turbulence interaction noise mechanism, as first described by Powell [7], further developed by Harper-

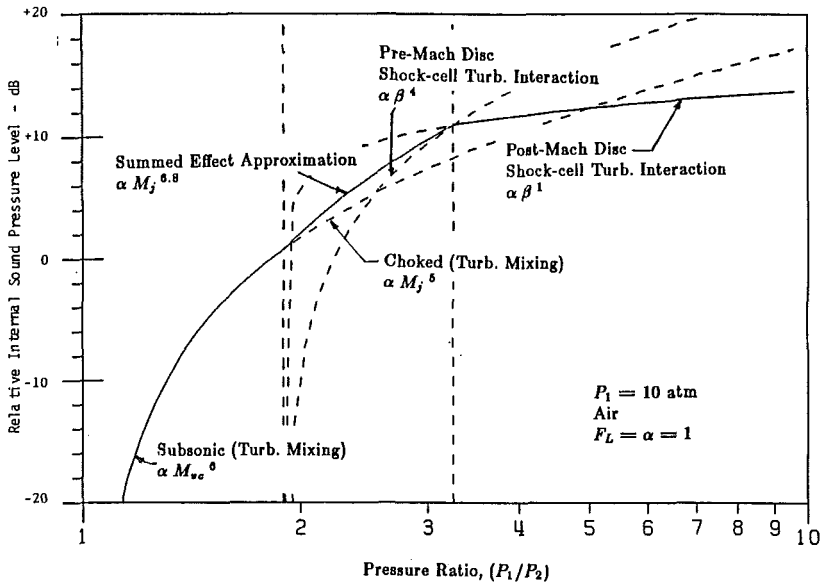

Fig. 3 Dependence of internal sound level on flow regime: turbulence, shock-turbulence interaction mechanisms

Bourne and Fisher [9] and recently refined by Seiner and Norum [8]. For valves, the sound power due to this mechanism can be expressed as:

$$W_{ac} = 1.1 \times 10^{-8} a_2^2 (M_j^2 - 1)^2 \left[1 \cdot a_2 C_V F_L \rho_1 \left(\frac{2}{\gamma + 1} \right)^{\frac{\gamma+1}{2(\gamma-1)}} \right] \quad (14)$$

where the quantity in brackets represents the choked mass flow. Above the pressure ratio at which $M_j = \sqrt{2}$, the shock cell structure becomes weaker, due to the formation of a Mach disk. This gives a fourth region to the sound power versus pressure ratio characteristic, which for air and $F_L = 1$ starts at a pressure ratio of 3.25. The acoustic power in this region is proportional to $(M_j^2 - 1)^{1/2}$ and is given by:

$$W_{ac} = 1.1 \times 10^{-8} a_2^2 (M_j^2 - 1)^{1/2} \left[1 \cdot a_2 C_V F_L \rho_1 \left(\frac{1}{\gamma + 1} \right)^{\frac{\gamma+1}{2(\gamma-1)}} \right] \quad (15)$$

Figure 3 shows a sample curve of the four mechanisms for the corrections shown.

Spectral Characteristics of Noise Generated by Valves

Since the pipe wall will be shown later to be a rather selective acoustic filter, it is necessary to break the overall acoustic power generated by the orificial elements of the valve into its spectral components. One-third octave band levels shall be used in the calculation procedures, overall the audible frequencies from the 200 Hz to the 20,000 Hz bands. The final procedure will involve combining sound pressure band levels with pipe wall transmission loss band levels, and, if needed, the spectral absorption characteristics of the space into which the pipe radiates. Finally, the A-weighted level will be calculated at the measurement point.

The spectra for valves operating at subcritical pressure ratios have a single marked peak, which is commonly expressed in terms of a nondimensional frequency called the Strouhal number, S_n, given by the ratio of frequency times jet diameter D_j divided by jet velocity V_j. For the subcritical case, and also the turbulent mixing dominated choked region, the peak amplitude occurs at a Strouhal number of 0.2, which agrees with free jet theory and experiment. Thus the peak frequency f_p for the subcritical region is given by

$$f_p = \frac{0.2\, M_{vc} a_2}{D_j} \quad (16)$$

For conventional valves, the characteristic dimension D_j is given by:

$$D_j = 0.0046 \left(\frac{C_V F_L}{n_o} \right)^{1/2} \quad (17)$$

The valve industry also uses a trim coefficient, F_d, which has been defined as:

$$F_d = \left(\frac{1}{n_o} \right)^{1/2} \quad (18)$$

The characteristic dimension then becomes:

$$D_j = 0.0046 (C_V F_L)^{1/2} F_d \quad (19)$$

For the shock cell–turbulence interaction caused noise, the peak frequency is obtained by calculating the time rate with which pressure disturbances are convected through successive stationary shock cells. Based on both theoretical and experimental work on free jets and valves, in both the strong shock cell regime and the high-pressure ratio, weak shock cell regime, an expression for the peak frequency shall be used which is in effect the ratio of disturbance convection velocity and shock cell spacing:

$$f_p = \frac{0.4 a_2}{1.25 D_j (M_j^2 - 1)^{1/2}} \quad (20)$$

Tests have confirmed the theory, for dipole sources, that spectrum roll-off occurs at f^4 below and f^{-2} above the peak frequency. The transition from the peak frequency to the two flanks is obtained by fitting suitable equations between the peak frequency and the flanks. The relationship which has been used to calculate each one-third octave band is given by

$$L_W(f_i) = L_{W_{\text{in}}}(0.A.) - 5.3 - 10 \log_{10} \left[1 + \left(\frac{f_i}{2 f_p} \right)^2 \right] \left[1 + \left(\frac{f_p}{2 f_i} \right)^4 \right] \quad (21)$$

where f_i are the one-third octave band center frequencies for the respective $i = 1$ to $i = 21$ bands. The logarithmic sum of all the L_W's will be equal to the overall sound power level inside the pipe.

Throughout the analysis it has been assumed that perfect gas relationships are valid. Should operation of the valve occur near the critical conditions, the ratio $P/\rho RT$ is no longer constant and equal to 1, and the ratio of specific heats γ is also affected. For steam, petrochemical gases, and other organic gases, corrections will become important to assure reliable noise prediction. The required correction relationships can be obtained from the thermodynamics literature and should be used to calculate the correct speed of sound and ratio of specific heats.

Propagation of Sound Inside the Pipe With Flow

Research has shown that, from the orifice of the valve to about 6 effective orifice diameters downstream, disturbances travel at the convection velocity of the stream. In this region the acoustic field develops. Beyond this region, the acoustic field is fully developed and disturbances propagate at the acoustic velocity of the medium, traveling essentially unattenuated down the pipe in a very complex manner [10]. Since typical industrial applications contain expansions, elbows, tees and other valves, acoustic reflections will exist, which in turn result in standing waves. The analysis of the acoustic field in such situations usually becomes intractable. For this prediction method, the pipe downstream of the valve is assumed to be of constant diameter and infinitely long.

The solution to the wave equation for such cylindrical ducts has been well developed [11, 12]. A multiplicity of higher-order modes, called spinning modes, is excited by a broadband sound source. Each of these modes is characterized by a critical frequency called the "cutoff" frequency. For frequencies above the cutoff frequency, each mode will travel down the pipe unattenuated, with increasing group velocity (energy propagation) and decreasing phase velocity as frequency increases. Below the cutoff frequency the amplitude of each mode attenuates rapidly with distance. The solution of the wave equation in cylindrical coordinates, with the imposition of hard-walled boundary conditions (zero radial velocity condition at the wall), defines the characteristic radial wave number k_{mn} and permits the development of the following dispersion relationship:

$$k_x = \frac{-M_2 k - \sqrt{k^2 - (1 - M_2^2) k_{mn}^2}}{1 - M_2^2} \quad (22)$$

where k_{mn} is the radial wave number for the mth circumferential and nth radial mode.

One of the more important assumptions of this analysis is that the pipe wall flexural vibrations do not affect the internal acoustic field, yet the acoustic field does uniquely determine the flexural excitation of the pipe wall. This assumption of separability is valid for the widely differing acoustic im-

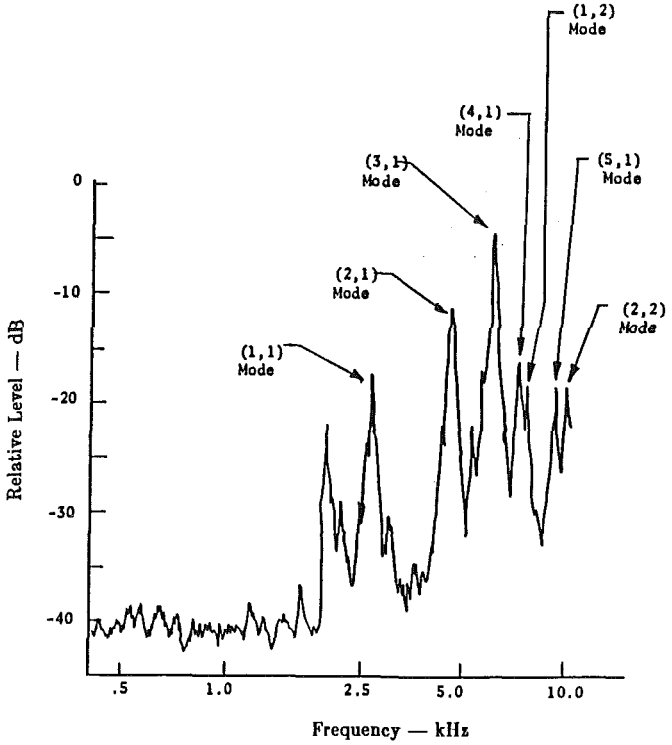

Fig. 4 Narrow band pipe wall acceleration spectrum of a 3-in. steel pipe.

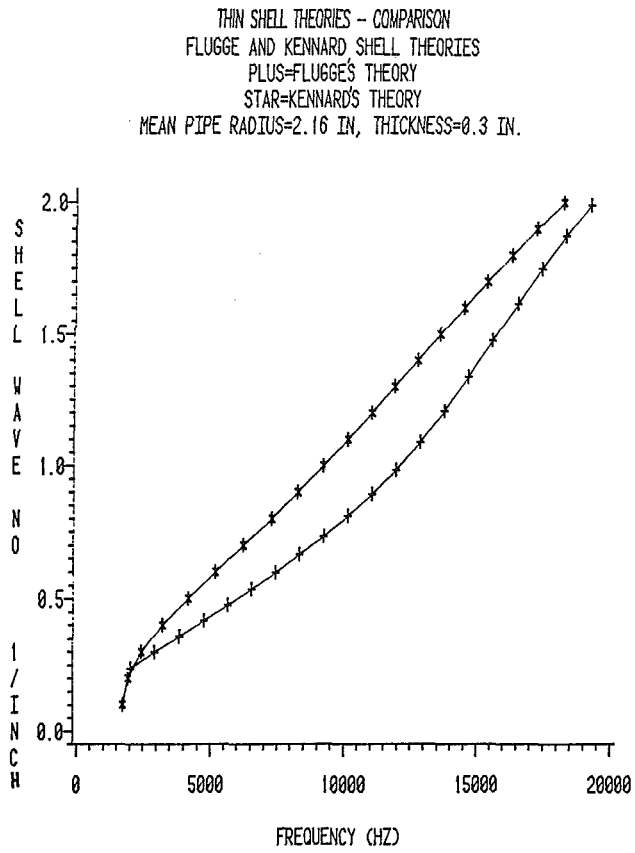

Fig. 5 Comparison of axial wavenumbers for Flugge and Kennard thin shell theories

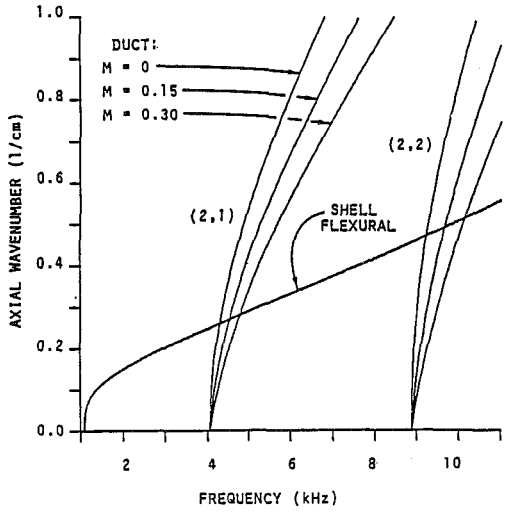

Fig. 6 Dispersion plot for the (2,1) (2,2) modes

pedances of steel pipe and gases even at high pressures, but breaks down for gases in PVC pipe or liquids in steel pipe [13].

The fluctuating pressures acting on the inside surface of the pipe must be calculated for each of the modes that is excited. It will be shown in the next section that the pipe wall responds at the coincidence frequencies of each acoustic mode (m, n) and the similar mth order pipe wall mode. It shall be assumed that the sound field is distributed uniformly across the pipe's internal area; in effect this corresponds to a plane wave approximation. The relationship between acoustic power and pressure is given by:

$$p^2 = \rho_2 a_2 W_{ac} / \pi r_p^2 \tag{23}$$

Pipe Wall Vibratory Response

The internal acoustic field, acting radially on the inside wall of the pipe, will excite a multiplicity of pipe wall normal flexural modes. For each acoustic spinning mode, there is a similar pipe wall vibratory mode which may exhibit a match in its axial phase velocity at a particular frequency. The phase velocity equality requires an equality of axial wave numbers, a condition termed coincidence. At the coincidence frequency, it can be shown that the acoustic pressure field and transverse bending motions remain in phase over long axial distances, interacting constructively as they propagate. At all other frequencies above the coincidence frequencies, the two waves quickly go out of phase, interfering destructively and resulting in little if any pipe wall motion. Therefore, significant acoustic energy from inside the pipe is *only* transmitted at the coincidence frequencies.

The results of pipe wall acceleration measurements on a long, straight, 3-in. schedule 40 steel pipe, with a globe valve as a noise source, are given in Fig. 4. The 20-Hz bandwidth spectrum clearly shows that the spectrum is dominated by the energy transmitted at the coincidence frequencies of, for example, the (3,1) mode. The peaks are as much as 25 dB higher than the broadband levels. Precise frequency measurements of the peak frequencies have consistently shown that the peaks do occur at exactly the respective modes' coincidence frequencies [14]. For smaller pipe sizes, such as the 3-in. pipe (shown in Fig. 4) the number of coincidence conditions is very low, indicating that one-third octave levels will be clearly dominated by only one coincidence. As pipe size increases, the modal density (the number of coincidence conditions per unit frequency), increases markedly. Thus a 2-in. schedule 80 pipe has only 6 coincidences for frequencies up to 20,000 Hz, whereas an 8-in. schedule 40 pipe has 68 such coincidences.

The analytical expressions for the pipe wall vibrational response are based on thin shell theory. The assumptions of this theory are:

1 The thickness of the shell is restricted to values of thickness to diameter ratios less than 1/10 to 1/20.

Table 1

TRANSMISSION LOSS VALUES IN ANSI STEEL PIPES (DB)

(STANDARD AIR, MACH NO = 0.0)

THIRD OCTAVE CENTER FREQUENCY, HZ

PIPE SIZE In.	SCHEDULE	THICKNESS In.	* 200*	250*	315*	400*	500*	600*	800*	1000*	1250*	1600*	2000*	2500*	3150*	4000*	5000*	6300*	8000*	10K*	12.5*	16K*	20K*
1	40	0.133	87.6	85.6	83.6	81.6	79.6	77.6	75.6	73.6	71.6	69.6	67.6	65.6	63.6	61.6	59.6	57.6	55.6	59.9	61.8	63.9	65.9
1	80	0.179	92.9	90.9	88.9	86.9	84.9	82.9	80.9	78.9	76.9	74.9	72.9	70.9	68.9	66.9	64.9	62.9	60.9	61.5	64.4	66.5	68.5
1	160	0.250	94.9	92.9	90.9	88.9	86.9	84.9	82.9	80.9	78.9	76.9	74.9	72.9	70.9	68.9	66.9	64.9	62.9	60.9	74.3	69.4	71.4
2	40	0.154	78.6	76.6	74.6	72.6	70.6	68.6	66.6	64.6	62.6	60.6	58.6	56.6	54.6	52.6	55.1	56.1	61.6	61.1	63.7	62.7	64.7
2	80	0.218	83.3	81.3	79.3	77.3	75.3	73.3	71.3	69.3	67.3	65.3	63.3	61.3	59.3	57.3	59.4	58.3	58.0	64.2	65.2	66.5	64.1
2	160	0.343	86.4	84.4	82.4	80.4	78.4	76.4	74.4	72.4	70.4	68.4	66.4	64.4	62.4	60.4	58.4	64.1	66.2	68.1	72.8	69.9	72.9
3	40	0.216	77.7	75.7	73.7	71.7	69.7	67.7	65.7	63.7	61.7	59.7	57.7	55.7	56.3	56.1	56.1	60.1	62.7	63.0	62.1	63.5	66.3
3	80	0.300	79.6	77.6	75.6	73.6	71.6	69.6	67.6	65.6	63.6	61.6	59.6	57.6	55.6	59.0	56.0	62.9	64.7	65.8	62.7	68.1	70.1
3	160	0.437	80.9	78.9	76.9	74.9	72.9	70.9	68.9	66.9	64.9	62.9	60.9	58.9	56.9	62.2	64.2	66.2	81.2	69.1	69.8	71.3	77.9
4	40	0.237	72.8	70.8	68.8	66.8	64.8	62.8	60.8	58.8	56.8	54.8	52.8	58.9	57.7	57.7	52.6	62.1	62.4	58.9	60.5	61.3	66.9
4	80	0.337	78.5	76.5	74.5	72.5	70.5	68.5	66.5	64.5	62.5	60.5	58.5	56.6	97.5	56.8	61.9	63.7	64.6	63.3	65.0	65.1	70.2
4	160	0.531	79.0	77.0	75.0	73.0	71.0	69.0	67.0	65.0	63.0	61.0	59.0	57.0	61.9	63.9	65.9	69.7	68.4	70.7	70.4	69.9	75.7
6	40	0.280	70.6	68.6	66.6	64.6	62.6	60.6	58.6	56.6	54.6	53.8	52.3	54.1	53.6	60.2	60.0	58.3	59.6	58.8	59.3	62.1	66.9
6	80	0.432	72.1	70.1	68.1	66.1	64.1	62.1	60.1	58.1	56.1	54.1	56.1	55.5	60.1	63.3	63.4	61.5	65.9	63.5	63.9	66.9	71.3
6	160	0.718	74.3	72.3	70.3	68.3	66.3	64.3	62.3	60.3	58.3	56.3	69.1	62.5	64.5	66.5	67.5	68.7	69.9	68.8	71.1	72.2	77.5
8	40	0.322	66.6	64.6	62.6	60.6	58.6	56.6	54.6	52.6	54.8	61.3	54.7	54.0	60.0	59.9	57.4	56.3	57.9	59.4	59.9	61.5	66.9
8	80	0.500	75.5	73.5	71.5	69.5	67.5	65.5	63.5	61.5	54.2	55.4	55.8	59.3	61.9	62.4	61.6	62.9	63.1	63.9	64.7	67.0	71.8
8	160	0.906	72.0	70.0	68.0	66.0	64.0	62.0	60.0	58.0	56.0	60.6	62.5	64.5	70.2	67.7	69.1	69.3	69.3	71.7	71.7	74.7	79.4
10	40	0.365	64.3	62.3	60.3	58.3	56.3	54.3	52.3	54.2	61.8	54.1	53.7	52.4	59.1	57.1	53.6	56.6	57.7	59.0	60.6	62.4	67.1
10	80	0.593	75.3	73.3	71.3	69.3	67.3	65.3	63.3	53.9	54.8	55.7	58.9	61.6	61.9	59.7	61.3	62.1	63.6	64.9	66.1	68.2	72.9
10	160	1.125	70.0	68.0	66.0	64.0	62.0	60.0	58.0	56.0	60.3	62.5	64.4	74.3	66.9	69.3	69.3	68.8	71.6	72.0	74.0	75.7	81.1
In.		In.	* 200*	250*	315*	400*	500*	600*	800*	1000*	1250*	1600*	2000*	2500*	3150*	4000*	5000*	6300*	8000*	10K*	12.5*	16K*	20K*
12	40	0.406	62.7	60.7	58.7	56.7	54.7	52.7	50.7	49.6	52.5	54.3	52.0	57.5	56.9	55.7	56.8	56.4	58.5	60.4	60.9	62.8	68.1
12	80	0.687	64.9	62.9	60.9	58.9	56.9	54.9	52.9	54.1	54.6	53.1	60.3	62.4	60.3	64.2	60.6	62.0	64.4	65.2	66.9	68.9	73.8
12	160	1.312	70.0	68.0	66.0	64.0	62.0	60.0	58.0	61.5	61.7	63.8	65.8	66.7	67.8	69.9	67.9	70.5	71.9	73.8	74.8	77.0	81.2
14	40	0.438	59.9	57.9	55.9	53.9	51.9	49.9	58.3	58.0	54.5	54.0	53.2	58.9	55.6	55.7	56.2	57.3	58.9	60.6	61.2	63.5	69.4
14	80	0.750	65.4	63.4	61.4	59.4	57.4	55.4	56.0	54.9	55.8	54.0	62.0	62.1	58.3	61.3	62.4	63.2	65.0	65.7	67.5	69.5	76.0
14	160	1.406	68.4	66.4	64.4	62.4	60.4	58.4	56.4	60.3	62.3	64.4	68.4	67.4	69.1	69.6	69.0	71.0	72.1	73.2	74.8	77.2	82.5
16	40	0.500	60.6	58.6	56.6	54.6	52.6	50.6	49.4	52.4	54.1	52.1	57.6	57.0	54.4	55.8	56.4	58.7	59.8	61.4	62.0	65.2	73.1
16	80	0.844	62.7	60.7	58.7	56.7	54.7	52.7	54.0	54.7	54.0	59.9	62.7	60.3	60.1	61.5	62.8	63.8	65.2	67.3	68.2	70.8	80.6
16	160	1.594	67.4	65.4	63.4	61.4	59.4	57.4	61.9	57.2	61.3	65.5	66.6	68.0	69.1	67.7	70.4	71.4	73.6	75.2	76.4	78.6	86.1
18	40	0.562	57.9	55.9	53.9	51.9	49.9	59.4	55.7	55.8	53.9	53.8	58.5	55.7	54.2	56.0	57.7	58.5	60.8	62.3	63.0	67.9	84.6
18	80	0.938	62.8	60.8	58.8	56.8	54.8	56.6	66.4	56.4	54.9	62.2	62.3	58.9	60.7	61.0	63.4	64.5	65.8	68.0	68.9	74.1	101.0
18	160	1.781	66.6	64.6	62.6	60.6	58.6	56.6	60.5	56.7	64.3	66.7	66.9	69.0	69.0	69.4	71.1	71.6	74.9	75.7	76.6	81.4	104.0
20	40	0.594	57.9	55.9	53.9	51.9	49.9	48.8	52.2	56.1	51.7	56.9	56.3	55.2	55.0	56.3	58.5	59.5	61.1	62.3	64.1	71.8	78.9
20	80	1.031	60.3	58.3	56.3	54.3	52.3	53.6	54.9	56.3	57.8	62.7	60.0	60.2	61.1	62.8	63.8	65.4	67.2	68.6	70.4	80.7	83.7
20	160	1.969	66.9	64.9	62.9	60.9	58.9	60.2	58.5	61.4	65.2	66.5	67.2	69.5	67.6	70.5	71.4	73.0	74.0	76.7	77.5	85.7	89.3
24	40	0.688	55.0	53.0	51.0	49.0	48.1	52.3	62.0	53.2	54.0	56.6	56.0	56.2	55.2	57.6	58.7	59.8	61.6	63.1	68.4	100.6	80.2
24	80	1.219	58.4	56.4	54.4	52.4	62.7	56.8	58.3	56.7	62.4	60.4	61.8	60.9	62.2	63.8	64.9	66.1	67.7	69.6	76.2	83.2	85.1
24	160	2.344	62.8	60.8	58.8	56.8	57.3	64.7	58.8	64.8	65.5	66.1	69.6	67.6	69.6	71.5	72.4	74.4	76.3	77.5	82.4	88.9	90.8

Note to Table 1: This table is based on standard air. Accuracy at higher downstream pressures can be improved through use of a modified transmission loss defined below:

$$L_{TL}(f_i)_{\text{mod}} = L_{TD}(f_i)_{\text{tab}} + 10\log_{10}\left[\frac{408(1+P_2/10^5)+4.93tfi}{816+4.93tfi}\right] - 10\log_{10}[G(\mathrm{M}_2)]$$

(Symbols and their units are as defined in the body of the paper. $G(\mathrm{M}_2)$ is found from equation (32) for downstream Mach numbers greater than zero.)

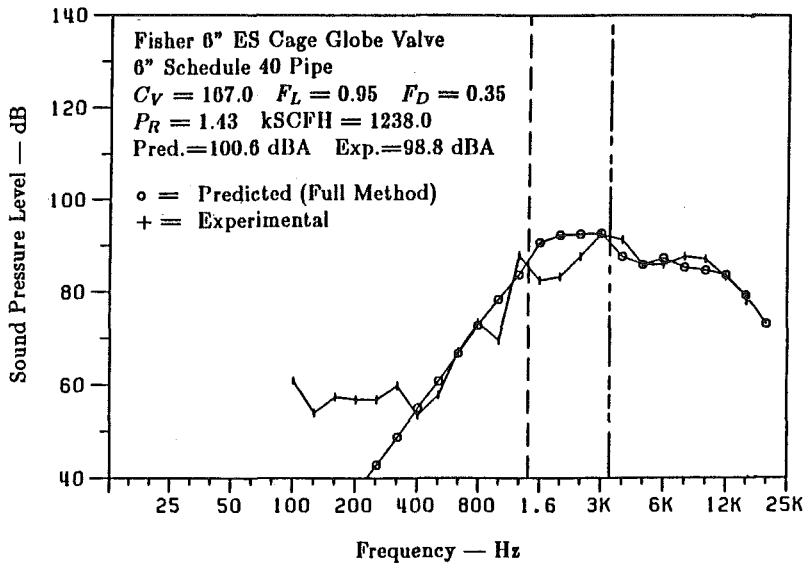

Fig. 7 One-third octave sound pressure levels at 3 ft from pipe wall for a 6-in. cage-glove valve

2 The material is linearly elastic, isotropic and homogeneous.

3 The displacements are assumed to be small relative to the pipe thickness.

4 Normal stress in the shell is negligible compared to the plane stresses.

5 The Euler hypothesis that perpendicular deflection lines will remain perpendicular and unstrained is considered valid.

6 Higher-order terms in the strain-displacement relationship can be neglected.

7 Shear deformations and rotary inertia effects are neglected.

These relationships are based on the well-known Flügge's thin shell theory [15].

The three differential equations of motion for the thin cylindrical shell, in the cylindrical coordinates x, θ, and r, can be written in matrix form, as given in equation (24)

$$[\mathbf{L}]\{\mathbf{U}_i\} = [\mathbf{0}] \tag{24}$$

where $\{\mathbf{U}\}_i$ is the displacement vector in the u, v, and w coordinates, and [L] is the matrix differential operator given in Appendix A.

The differential equation is solved for the axial wave number k_x by assuming a harmonic time dependence for the displacements, of the form of equations (25)

$$u = B_1 \cos(k_{xs}x)\cos(m\theta); v = B_1\delta_1 \sin(k_{xs}x)\sin(m,\theta);$$

$$w = B_1\delta_1 \sin(k_{xs}x)\cos(m,\theta) \tag{25}$$

These relations are substituted into equation (24). After taking suitable derivatives and using the following dimensionless parameters:

$$\epsilon = h\,k_x;\ \beta = h/r;\ \Omega = \omega h\sqrt{\rho(1-\nu^2)/\mathrm{E}} \tag{26}$$

The differential equations are thereby reduced to a set of three algebraic equations, which can be written in matrix form, as in equation (27)

$$\begin{bmatrix} \mathbf{A}_{11}\mathbf{A}_{12}\mathbf{A}_{13} \\ \mathbf{A}_{21}\mathbf{A}_{22}\mathbf{A}_{23} \\ \mathbf{A}_{31}\mathbf{A}_{32}\mathbf{A}_{33} \end{bmatrix} \begin{bmatrix} 1 \\ \delta_1 \\ \delta_2 \end{bmatrix} = \begin{bmatrix} 0 \\ 0 \\ 0 \end{bmatrix} \tag{27}$$

The terms of the A matrix are given in Appendix B. This matrix gives the important characteristic (or eigen) equation, which permits the structural wave number k_{xs} to be determined as a function of frequency for each mode m. Figure 5 shows an example of a shell wave number dispersion plot for mode 1. Solutions to a simplified form of Flügge's equations, due to Kennard [16, 17], are also shown on the figure. Kennard neglected second-order thickness terms in the shell equations of motion; therefore, Flügge's formulation should provide more accurate results, particularly for pipes with thicker walls. This fact has been mentioned because Fagerlund's work [18, 19] on transmission loss in pipes is based on Kennard's approximation. The need for Flügge's more complex formulation has been questioned on several occasions; however, Kennard's theory will often give higher wave number values (and thus higher coincidence frequencies).

The dispersion relationship for the internal acoustic field, given in equation (22) can, for particular circumferential modes m and radial modes n, be combined with a dispersion relation of the similar pipe wall flexural mode, also of order m, on a plot of axial wave numbers, k_x and k_{xs}, versus frequency. An example is given in Fig. 6 for the second circumferential mode ($m=2$) and two radial acoustic modes ($n=1$ and $n=2$) for a 3-in. pipe. The effect of convection velocity of the gas in the pipe is also shown on the acoustic dispersion plot, for Mach number values of M = 0, 0.15, and 0.30. The coincidence frequencies are obtained by determining the intersection of the appropriate dispersion relationships, using an iterative procedure.

From equation (27) it can be seen that the acoustic dispersion characteristic is dependent on the wave number k, which is inversely proportional to the speed of sound (a_2) in the pipe. Thus, for $M_2 = 0$,

$$k_x = \sqrt{{a_2}^2\omega^2 - {k_{mn}}^2}. \tag{28}$$

where $a_2 = \sqrt{\gamma R T_2}$. At cutoff, $k_x = 0$ and $\omega_{co} = a_2 k_{mn}$. Therefore, the acoustic dispersion plots are functions of gas properties and gas temperature. The coincidence frequencies will shift to higher values with increasing gas temperature. It is necessary, therefore, to include gas properties γ and R, as well as gas temperature, in the formulation of the dispersion relationship.

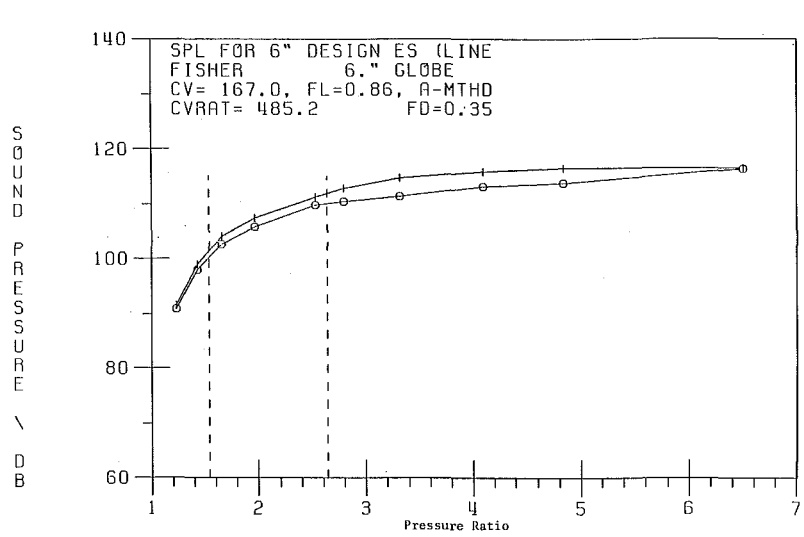

Fig. 8 Overall (*A*-weighted) sound pressure level comparison for a 6-in. cage globe valve at 3 ft downstream of valve and 3 ft away from pipe

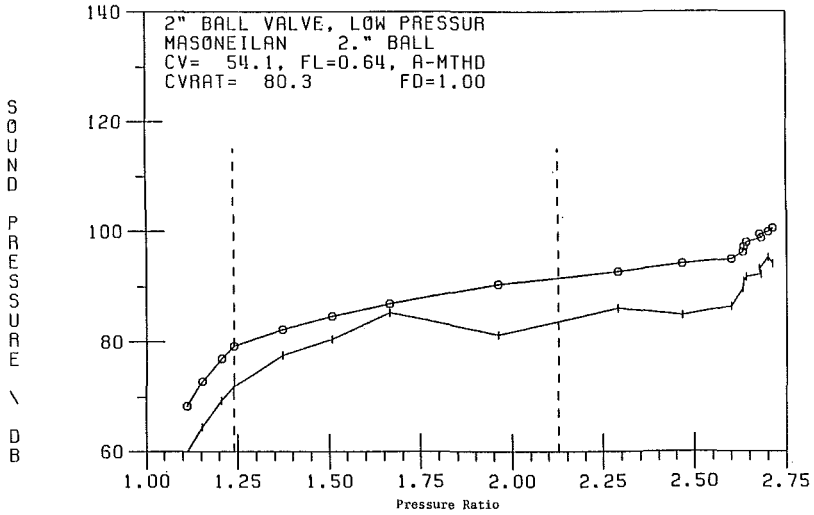

Fig. 9 Overall (*A*-weighted) sound pressure level comparisons for a 2-in. semi-spherical ball valve at 3 ft downstream of valve and 3 ft away from pipe

Transmission Loss Relationship

General Considerations. The transmission loss through the walls of a pipe is defined as 10 times the logarithm (base 10) of the ratio of acoustic energy inside the pipe to the energy in the external acoustic field. Several modes of transmission exist, depending on frequency regimes and dynamic characteristics of the acoustic field–pipe wall vibratory mode interaction. At frequencies below the first coincidence frequency, where energy propagation can occur only in plane wave ([0, 0]) modes, the transmission is controlled by stiffness. Above the first coincidence frequency, the transmission through the pipe wall is dominated by the subsequent coincidence conditions, which can be likened to resonances. Between coincidences, it is assumed that the transmission is controlled by the mass law. In terms of mechanical impedance concepts:

$$Z_m = R_m - j\left(\omega m_e - \frac{K}{\omega}\right) \tag{29}$$

The energy transmitted is related to the square of the impedance; thus, in the stiffness controlled, low frequency region, the transmission loss is inversely proportional to the square of increasing frequency, and in the mass controlled region, transmission increases proportional to frequency squared. In terms of decibel measures, the transmission loss decreases in the stiffness controlled region by 6 dB per halving of frequency, and increases at the rate of 6 dB per doubling of frequency for mass controlled regions.

The four general classes of solution methods to vibrating system are the classical, the statistical energy, the finite element, and the integral transform methods. The use of a combination of classical and statistical energy methods will reduce the analytical complexities to manageable levels. The combined method is based on the work of Walter [12], Szechenji [20], Holmer and Anderson [21], Fahy [22], Mani [23] and is largely an adaption of Fagerlund's procedure [18, 19].

Transmission Loss Calculations. A relationship for each of the terms in the energy balance equation can be developed [18, 19], and the structural to acoustic energy ratio can be obtained, providing an expression for the transmission loss L_{TL} equation (30) for each frequency band:

$$L_{TL}(f_i) = 10 \log \left[\frac{18\rho_s r_p^2 h \omega_i^2 \Delta\omega_i}{5\rho_o{}^2 a_o{}^2 a_2^2 d} \cdot \frac{(\rho a_2 \sigma + \rho_o a_o \sigma_o + h\rho_s \omega_i \eta_s)}{(\Delta k_{xsi}) G(\mathrm{M}) \sigma \sigma_o} \right] \quad (30)$$

This general transmission loss relationship utilizes the internal and external gas properties, the pipe diameter and thickness, and the sum of the changes in the structural wave numbers, Δk_{xsi}, which occur after each coincidence and within a frequency band of width $\Delta\omega$ and center frequency ω_i. The value of Δk_{xsi} is obtained for each coincidence from the previously discussed dispersion plots. It shall be assumed that radiation efficiencies are unity above the coincidence frequencies, up to the upper frequency of the one-third octave band struck about the coincidence frequency, and zero elsewhere. This assumption can be justified for one-third octaves, but may result in significant errors for wider or narrower bands. If this upper frequency is higher than the limit of the *standard* one-third octave band which contains the coincidence, the spillover is added to contributions from the coincidences in the next higher band.

The convection correction factor $G(\mathrm{M})$ is given by equation (31):

$$G(\mathrm{M}) = \frac{12}{\mathrm{M}^3} \left(\frac{1+\mathrm{M}}{2+\mathrm{M}} \right) \left[\frac{\mathrm{M}}{2} \left(\frac{2-\mathrm{M}}{1-\mathrm{M}} \right) + \ln(1-\mathrm{M}) \right] \quad (31)$$

The one-third octave band transmission losses for pipe sizes ranging from 1 in. to 24 in. and the most common schedules have been calculated for convection velocities of zero and Mach 0.3. Table 1 is a sample of this result for 3 in. schedule 40 pipe and a Mach number of 0.3. The downstream pipe conditions are 14.7 psi and 68°F; the gas is air. The table also contains a correction for differences in downstream density.

An increase (decrease) in the speed of sound compared to air at standard conditions will shift the coincidence frequencies upward (downward), changing the Δk_{xs} distributions in the one-third octave bands. Thus a significant change in L_{TL} will occur; hence in order to fully account for changes in sound speed, a complete recalculation is required.

Radiation From the Pipe Wall. The methods described in the previous sections calculate, in one-third octave bands, the power generated by the valve's orificial element, the conversion of that power to a fluctuating pressure at the inner surface of the pipe wall, and the transmission loss resulting in the sound pressures at the outer surface of the pipe wall. If the pipe is assumed to act as an infinitely long cylindrical radiator, radiating into a free field, the sound pressure levels at a distance (m) from the center of the pipe can be calculated by

$$L_s = L_a - 10 \log_{10} \left[\frac{s}{r_p} \right] \quad (32)$$

The A weighted level is then obtained in the usual manner.

Verification of Prediction Method. The accuracy of the comprehensive theoretically based prediction method has been tested by comparing the calculated sound pressure levels, for several styles of conventional valves, with actual test data provided by several major valve manufacturers. The test data are in one-third octave band sound pressure levels at a number of pressure ratios, ranging from subcritical (such as $P_1/P_2 = 1.12$) to high-pressure ratios of 14 in the choked region. The complete method was programmed on the Penn State College of Engineering's VAX 11/780 minicomputer. A typical comparison resulting from a 6-in. cage-globe valve, is shown in Fig. 7. Satisfactory agreement over the whole spectrum is indicated. The slopes of the skirts below and above the peak frequency are well reproduced. The overall values on the A weighting have a better than 2-dB agreement.

Figure 8 gives comparisons on the same 6-in. valve with pressure ratios ranging from 1.43 to 6.8. Agreement appears quite satisfactory between prediction and test data with this and most cases lying within 2-dB differences. The prediction method has also been applied with favorable results to the swage-piping systems, for example, a 4-in. valve opening into an 8-in. downstream pipe. Figure 9 shows the results for a 2-in. semispherical ball valve. The predictions are consistently higher, by as much as 10 dB, for the 50 percent open valve, with the noise measurements deviating quite substantially from a smooth progression as pressure ratios increase. The agreement is somewhat better for the full open ball valve. It is suggested, based on the valve orifice configuration, that jet wall attachments and detachments occur, which could explain the somewhat erratic decrease in noise generation in this valve. The prediction method is of course not able to take account of any C_v and F_L uncertainties, significant friction or multiple flow direction changes. Of great concern are the effects of bistable flows due to wall attachment, the Coanda effect which has been observed in Schlieren studies [6]. Noise reductions of 8 to 10 dB have been noted as a result of wall attachment. The method provides reliable prediction for the much more common detached jets, and in fact predicts the maximum noise generation for this ball valve quite well.

Conclusions

A valve noise prediction method for compressible fluids have been developed which is based on analytical expressions which are derived from fundamental principles of fluid and applied mechanics. At this time, the method is limited to conventional type control valves as opposed to quiet trims with very complex throttling elements. Also, the downstream piping must have a reasonably long length of straight section without fittings. On the other hand, swage type installations are acceptable provided the resulting changes in C_v and F_L are incorporated.

The method predicts the one-third octave (or octave) band levels and the A-weighted sound levels at any location from the pipe in a free acoustic field.

The analytical details of the four pressure ratio regimes of sound generation, the calculation of the acoustic field inside the pipe, the pipe vibration characteristics, the resulting coincidence frequencies, and the resulting transmission loss calculations require the computation capabilities of a minicomputer.

For gases at a fixed sound speed, the method can be used with a hand-held programmable calculator, such as Hewlett-Packard HP 41 CV with magnetic card reader.

A large number of comparisons has been made between predicted A-weighted sound level and measurements provided by Fisher Controls Co. and Masoneilan International, wide pressure ratio ranges, for several valve styles and openings (lifts). With the exception of a ball valve, the agreement has been good with variations within ± 3 dB. The method has not been tested for high-temperature high-pressure steam, or gases other than air, because reliable data is simply not yet available. This fundamental-based valve noise predictiion method is a considerable improvement over the presently available methods, which are primarily based on empiricisms.

References

1 Reethof, G., "Turbulence Generated Noise in Pipe Flow," *Am. Rev. Fluid Mech.*, Vol. 10, 1978, pp. 33–67.

2 Reethof, G., "Control Valve and Regulator Noise Generation, Propagation, and Radiation," *Noise Control Engineering*, Vol. 9, No. 2, Sept. 1977, pp. 74–85.

3 Shea, Allan K., "A Comparative Study of Sound Level Prediction Methods for Control Valves," Master of Engineering Report, The Pennsylvania State University, Behrend Campus, Erie, PA, Aug. 1982.

4 Baumann, H. D., "How to Estimate Aerodynamic Valve Throttling Noise: A Fresh Look," presented at the ISA/82, Paper C182-902.

5 Baumann, H. D., "The Introduction of a Critical Flow Factor for Valve Sizing," *ISA Transactions*, Vol. 2, No. 2, Apr. 1963.
6 Chow, G. C., and Reethof, G., "A Study of Valve Noise Generation: Processes for Compressible Fluids," ASME Paper 80-WA/NC-15, 1980.
7 Powell, A., "On the Mechanism of Choked Jet Noise," *Proc. Phys. Soc. London*, Sect. B, Vol. 66, 1953, pp. 1039-1056.
8 Seiner, J. M., and Norum, T. D., "Experiments of Shock Associated Noise in Supersonic Jets," AIAA Paper 79-1526, July 23-25, 1979.
9 Harper-Bourne, M., and Fisher, M. J., "The Noise From Shock Waves in Supersonic Jets," AGARD CP-131 (11), 1973.
10 Reethof, G., and Karvelis, A. V., "Internal Wall Pressure Field Studies Downstream from Orificial-Type Valves," Paper 78-827, presented at ISA/74 Meeting, New York, NY, 1974.
11 Morse, P. M., and Ingard, K. U., *Theoretical Acoustics*, McGraw-Hill, New York, 1968.
12 Skudrzyk, E., *Foundations of Acoustics*, Springer-Verlag, New York, 1971.
13 Walter, J. L., McDaniel, O. H., and Reethof, G., "Excitation of Cylindrical Shell Vibrations as a Result of Pipe Wall-Acoustic Coincidence from Internal Sound Fields," ASME Paper 79-WA/DSC-25, Dec. 1979.
14 Walter, J. L., "Coincidence of Higher-Order Modes – A Mechanism of the Excitation of Cylindrical Shell Vibrations via Internal Sound," Ph.D. Thesis, The Pennsylvanis State University, 1979.
15 Flügge, W., *Static und Dynamik der Schalen*, Springer-Verlag, Berlin, 1934, pp. 115 and 230.
16 Kennard, E. H., "The New Approach to Shell Theory: Circular Cylinder," ASME *Journal of Applied Mechanics*, Vol. 22, No. 1, Mar. 1955, pp. 111-116.
17 Kennard, E. H., "Approximate Energy and Equilibrium Equations for Cylindrical Shells," ASME *Journal of Applied Mechanics*, Vol. 23, No. 4, Dec. 1956, pp. 645-646.
18 Fagerlund, A. C., and Chow, D. C., "Sound Transmission Through a Cylindrical Pipe Wall," ASME *Journal of Engineering for Industry*, Vol. 103, No. 4, Nov. 1981, pp. 355-360.
19 Fagerlund, A. C., Ph.D. Thesis, The University of Iowa, 1979.
20 Szechenji, E., "Sound Transmission Through Cylinder Walls Using Statistical Considerations," *Journal of Sound and Vibration*, Vol. 19, No. 1, 1971, pp. 83-94.
21 Holmer, C. I., and Anderson, D. W., "Transmission of Sound Through Pipe Walls as a Function of Flow Within the Pipe," presented at the 85th meeting of the Acoustical Society of America, Apr. 1973.
22 Fahy, F. J., "Response of a Cylinder to Random Sound in the Contained Fluid," *Journal of Sound and Vibration*, Vol. 13, No. 2, 1970, pp. 171-194.
23 Mani, A., "Acoustic Transmission Loss of Metal Pipes for Compressible Fluids," M.S. Thesis, Department of Mechanical Engineering, The Pennsylvania State University, May 1983.

APPENDIX A

Differential Operator [L] in Flügge's Formulation of the Thin Shell Equations

where

$$s = \frac{x}{R}$$

$$k = \frac{h^2}{12R^2}$$

$$[\mathbf{L}] = \begin{bmatrix} \frac{\partial^2}{\partial s^2} + \left(\frac{1-\nu}{2}\right)\frac{\partial^2}{\partial \theta^2} - \rho_s\left(\frac{1-\nu^2}{\mathrm{E}}\right)R^2\frac{\partial^2}{\partial t^2} & \left(\frac{1+\nu}{2}\right)\frac{\partial^2}{\partial s\partial\theta} & \nu\frac{\partial}{\partial s} - \frac{h^2\partial^3}{12R^2\partial s^3} + \frac{h^2\partial^3}{24R^2\partial s\partial\theta^2} \\ + \frac{h^2}{24R^2}(1-\nu)\frac{\partial^2}{\partial\theta^2} & & \\ \left(\frac{1+\nu}{2}\right)\frac{\partial^2}{\partial s\partial\theta} & \left(\frac{1-\nu}{2}\right)\frac{\partial^2}{\partial s^2} + \frac{\partial^2}{\partial\theta^2} - \frac{\rho_s(1-\nu^2)}{\mathrm{E}}R^2\frac{\partial^2}{\partial t^2} & \frac{\partial}{\partial\theta} - \frac{h^2(3-\nu)}{24R^2}\frac{\partial^3}{\partial s^2\partial\theta} \\ & + \frac{3(1-\nu)}{24R^2}h^2\frac{\partial^2}{\partial s^2} & \\ \nu\frac{\partial}{\partial s} - \frac{h^2}{12R^2}\frac{\partial^3}{\partial s^3} & \frac{\partial}{\partial\theta} - \left(\frac{3-\nu}{24R^2}\right)\frac{\partial^3}{\partial s^2\partial\theta} & 1 + \frac{h^2\nabla^4}{12R^2} + \rho_s\frac{(1-\nu^2)}{\mathrm{E}}R^2\frac{\partial^2}{\partial t^2} \\ + \frac{h^2(1-\nu)}{24R^2}\frac{\partial^3}{\partial^3\partial\theta^2} & & + \frac{h^2}{12R^2} + \frac{2k\partial^2}{\partial\theta^2} \end{bmatrix}$$

APPENDIX B

The Terms of the Characteristics Matrix to be Solved for the Wave Number-Frequency-Mode Relationships

$$A_{11} = \left\{-\epsilon^2 - \left(\frac{1-\nu}{2}\right)\left[1 + \frac{\beta^2}{12}\right]m^2\beta^2 + \Omega^2\right\}$$

$$A_{12} = \left\{\frac{1+\nu}{2}\right\}m\epsilon\beta$$

$$A_{13} = \left\{\epsilon\beta\left(\nu + \frac{\epsilon^2}{12}\right) - \frac{(1-\nu)^3}{24}\beta m^2\epsilon\right\}$$

$$A_{21} = A_{12}$$

$$A_{22} = \left\{-\left(\frac{1-\nu}{2}\right)\left(1 + \frac{\beta^2}{4}\right)\epsilon^2 - m^2\beta^2 + \Omega^2\right\}$$

$$A_{23} = \left\{-m^2\beta - \left(\frac{3-\nu}{24}\right)\beta^2\epsilon^2 m\right\}$$

$$A_{31} = \left\{\epsilon\beta\left(\nu + \frac{\epsilon^2}{12}\right) - \left(\frac{1-\nu}{24}\right)\beta^3 m^2\epsilon\right\}$$

$$A_{32} = A_{23}$$

$$A_{33} = \left\{-\beta^2\left[1 + \frac{\beta^2}{12}1 - 2m^2\right)\right] - \frac{1}{12}(m^2\beta^2 + \epsilon^2)^2 + \Omega^2\right\}$$